ANALYSIS OF ELECTRON CLOUD AT RHIC*

U. Iriso†, M. Blaskiewicz, P. Cameron, A. Drees, W. Fischer, H.C. Hseuh,
R.C. Lee, S. Peggs, L. Smart, G. Rumolo&, D. Trbojevic, and S.Y. Zhang.
BNL, Upton, NY 11973, USA; &GSI, Darmstadt, Germany

Abstract

Pressure rises with high intense beams are among the main luminosity limitations at RHIC. Observations during the latest runs show beam induced electron multipacting as one of the causes for these pressure rises. Experimental studies are carried out at RHIC using devoted instrumentation to understand the mechanism leading to electron clouds. In the following, we report the experimental electron cloud data and the analyzed results using computer simulation codes.

INTRODUCTION

Pressure rises with high intense beams are among the main luminosity limitations at RHIC [1] since Run-2 in 2001. Using the electron detectors installed in the ring during the summer shutdown in 2002, the pressure rise when injecting high intense beams could be correlated to electron clouds [2]. While the pressure rises at injection in the warm straight sections could be directly linked to beam induced electron multipacting, during ramping the pressure rises became an issue primarily in the Interaction Regions, where no clear diagnostics could be done. A quasi linear dependence with the total beam intensity for both beams was found for this pressure rise [3]. In this paper, the situation in the interaction regions is addressed using both simulations and experimental observations in Run-4. Pressure rises in these locations (especially PHOBOS) during Run-4 (2004) have been the main limiting factor at RHIC [4].
A single case of pressure rise in the cold arcs have been detected during Run-4. Although the consequences of electron cloud in the cold sections (pressure rise or heat load) have not been a limiting factor, the situation at these locations is adressed in the next sections.

SITUATION IN THE INTERACTION REGIONS

Compared to the single beam chambers, the problem in the interaction regions lies in the uneven bunch spacings created when two beams circulate in opposite senses in the same chamber. The situation is described in Fig. 1 for two beams, colliding at the Interaction Point (IP): in the IP, the bunch spacing is the same as for a single beam, but the bunch intensity doubles. Placed at a distance z from the IP, a yellow (blue) bunch is separated by $s_{b_1} = 2 \cdot z$ from a blue (yellow) bunch, which in turn is $s_{b_2} = s_b - 2 \cdot z$ from the next yellow (blue) bunch, where s_b is the bunch spacing for a single beam. For example, at 7.5 m (dotted line at Fig. 1) from the IP and for a bunch spacing of 216 ns (64 m), the two different bunch spacings seen at this location are 15 m (52 ns) and 49 m (164 ns). The situation is symmetric for $\pm z$.

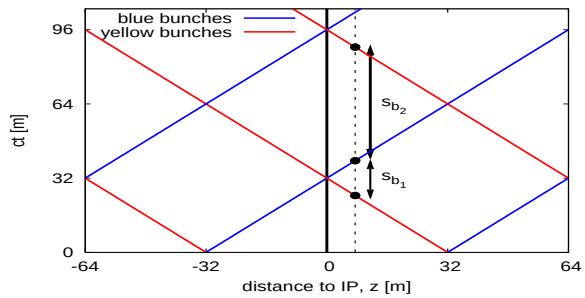

Figure 1: Bunch spacing seen by a point at a distance z from the IP when blue and yellow beams are colliding. In this case, we consider the case of a 64 m single beam bunch spacing (216 ns).

One of the main limitations during Run-4 has been the pressure rise and the experimental backgrounds at the PHOBOS experiment. Figure 2 shows an example of a high intensity fill producing pressure rises in PHOBOS (IR10) and STAR (IR6). The top plot shows the pressure behaviour while the ramping process takes place: the pressure increases by about a factor of 15 in IR10, and a factor 5 in IR6. Note that the pressure in IR10 evolves much more abruptly than in IR6. Pressure in IR10 has a pronounced spike when the beams cross the transition energy, then it calms down, and it suddenly increases again when the beams go through "rebucketing", a process in which, by means of an RF gymnastics, the bunches shrink to 4 ns full parabolic bunch lenght. The bottom plot in Fig. 2 shows the evolution of the beam intensity and the bunch length while this process takes place. Finally, after about one hour, the pressure in IR10 suddenly drops, in what we can call a first order phase transition [5]. On the other hand, the pressure at IR6 evolves more adiabatically: as the bunch length decreases, the pressure smoothly increases up to a factor of 5 after the "rebucketing" and smoothly decreases as the beam intensity decreases and the bunch length increases.

One of the reasons for this different behaviour is the different beam type material: whereas IR10 is made of Beryllium, IR6 is made of stainless steel baked only at 100 °C. The rest of the experimental areas are baked at a higher temperature. Unlike stainless steel, the Beryllium does not have a very clear SEY behaviour, especially after the beam

* Work performed under the auspices of the US Department of Energy
† ubaldo@bnl.gov

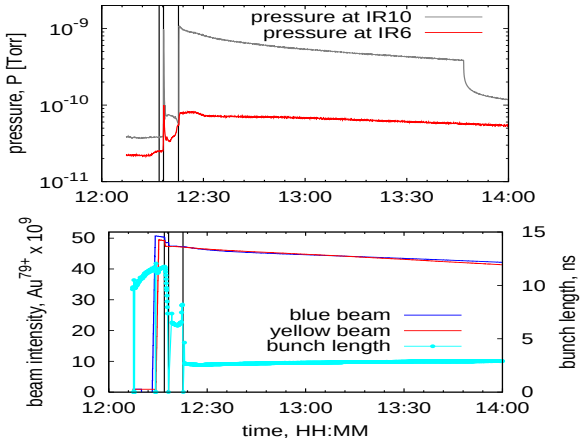

Figure 2: Pressure rise evolution at IR10, PHOBOS, and IR6, STAR, (top plot) when the ramping process starts (first vertical line, at 12:16:56), cross transition (second vertical line, at 12:18:14), and after rebucketing (at 12:22:38). The bottom plot shows the effect of these processes in the beam intensity and bunch lenght (light blue points).

pipe has suffered some scrubbing [4]. On the other hand, stainless steel is a well studied material, whose SEY parameters in the literature agree with the ones used in Table 1. In order to understand the pressure behaviour experienced in the IRs, we chose to launch different electron cloud simulations scanning both the bunch intensity and bunch length, using the parameters shown in Table 1. We decided to center the study placed at 7.5 m from IP6, since the vacuum gauges are at this location. The computer code used for these simulations is $CSEC$ [6].

Table 1: Input parameters for electron cloud simulations.

parameter	symbol	unit	value
bunch spacing	s_b	m	49/15
bunches	n	...	120
full bunch length	σ_z	ns	2 to 20
bunch charge	N	p·10^{10}	2 to 20
rms beam radius	r_b	mm	2
relativistic factor	γ	...	26
pipe radius	R	mm	37
reflection at energy$\rightarrow 0$	R_0	...	0.5
reflection at energy$\rightarrow \infty$	P_∞	...	0.1
reflection energy	E_{rf}	eV	60
rediffusion probability	P_{rd}	...	0.5
maximum SEY	SEY_{max}	...	2.0
energy for max. SEY	E_{max}	eV	325
energy for secondary e-	E_{sec}	eV	8.9

Figure 3 shows a contour plot of the saturated electron density as a function of bunch intensity, N, and bunch length, σ_z at 7.5 m from the IP at IR6. One can see that when injecting gold ions ($N = 10^9 \cdot Au^{79+}$, same charge as $7.9 \cdot 10^{10}$ protons, $\sigma_z = 18\ ns$), we are in a "free electron cloud region". However, as the bunch length is reduced, and if the bunch intensity does not decrease by more than about 25%, the electron cloud will be present and so the pressure rise after rebucketing can be explained ($N = 10^9 \cdot Au^{79+}$, $\sigma_z = 4\ ns$).

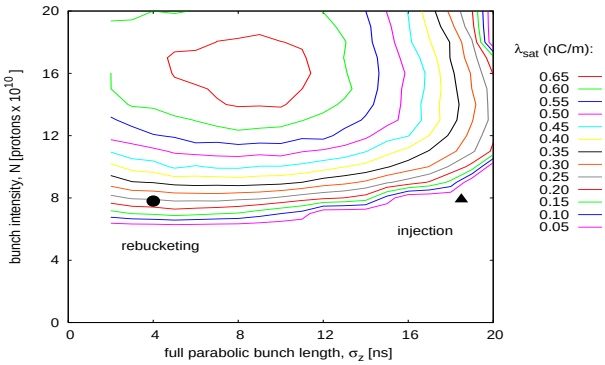

Figure 3: Map of the saturated electron cloud density scanning the bunch length and bunch intensity at 7.5 m from IP6. Although at injection (black triangle) the beams are in an electron cloud-free region, but as the bunches shrink they enter dangerous regions (rebucketing is marked with a black circle).

It is notable that the saturated electron density evolves from "off" to "on" in a smooth way (equispaced distance between curves marking the different levels of electron density), rather than in a "first order phase transition" mode. A similar study for the PHOBOS surface parameters is currently being carried out in order to enlighten this discussion. The polarization of a one meter long quadrupole, placed at 0.6 m to IP10 has recently been found to influence the pressure rise.

SITUATION IN THE COLD REGIONS

The main difference influencing the build up of an electron cloud in the cold regions as compared to the warm straight sections is the smaller beam pipe radius (in average, this is 3.5 vs 6 cm). Other differences, like the lower pressure (due to larger pumping speed of the cryopumps) and lower temperature are not taken into account in this study. The sensitivity of the cryosystem is limited to 150 W[6], which, given the typical RHIC parameters, is not be achieved by the electron cloud. Therefore, it has been thought that electron cloud can exist in the arcs, but it is hard to detect since its consequences are not "observable". As used in [6], one can use tune measurements along the bunch train to estimate an average electron density in the ring. This study was carried out during a dedicated beam experiment. Figure 4 (bottom) shows an injection consisting of 56 bunches with an average bunch charge, N of $1.6 \cdot 10^{11}$ protons spaced by 108 ns. The top plot in Fig. 4 shows the measured fractional tune of the last two bunches injected. That is, the last two bunches in the bunch train. One can see that the horizontal tune shift between the head

and the tail is about 0.002, while the vertical tune shift is ≤ 0.001.

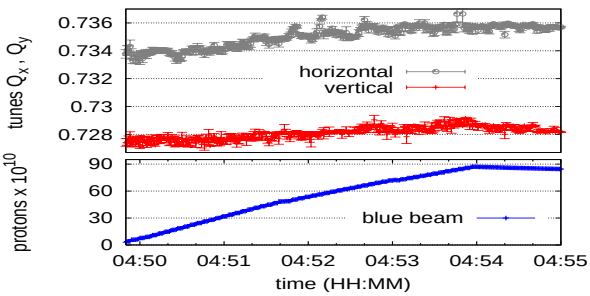

Figure 4: Horizontal and vertical tune measured with the PLL of the last two bunches as these are injected. The total beam injected is shown at the bottom plot. Note the slight assymetry between the vertical and horizontal data.

The formula for the tune shift produced by a linear electron density, λ uniformly distributed along a round beam chamber of radius R is [6]

$$\Delta Q = \frac{r_p}{\gamma} \oint \frac{\beta \cdot \lambda}{\pi \cdot R^2} dz \approx \frac{r_p}{\gamma} \sum \frac{\bar{\beta}_i \cdot \bar{\lambda}_i \cdot L_i}{\pi \cdot \bar{R}_i} \quad , \qquad (1)$$

where r_p stands for the classical proton radius, γ is the relativistic factor, β is the beta function ($\beta_x = \beta_y$ for round beams). The subindex i stands for the different parts of the rings. For our purposes, we separate the ring in two different parts: warm straight sections, and cold regions. With this approximation, Eq. 1 is:

$$\Delta Q = \frac{r_p \bar{\beta_w} L_w}{\gamma \pi \bar{R}_w^2} \cdot \bar{\lambda}_w + \frac{r_p \bar{\beta_c} L_c}{\gamma \pi \bar{R}_c^2} \cdot \bar{\lambda}_c \equiv \kappa_w \bar{\lambda}_w + \kappa_c \bar{\lambda}_c, \quad (2)$$

where the subindex w (c) states for the value of the corresponding magnitude in the warm (cold) region. Given

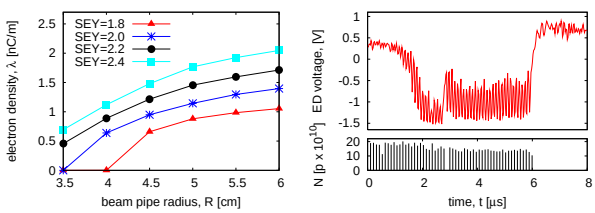

Figure 5: Saturated electron density as a function of the chamber radius (left hand side plot), and electron signal (right hand side figure, top plot) in the electron detector while injecting the 56 bunches whose bunch intensity can be seen in the bottom plot of the right hand side figure.

the typical RHIC parameters for the proton run at injection, the ratio $\kappa_c/\kappa_w$is $\approx$10. This case has been simulated using $CSEC$, scanning the value of SEY_{max} from 1.8 to 2.4. Figure 5 shows the saturated electron density as a function of the chamber radius for different SEY_{max}. Taking into account that the cold surfaces have not been baked and are barely scrubbed, typical $SEY_{max} \geq 2.1$. On the other hand, $\approx$ 90% of the warm parts have been baked (and probably scrubbed) and typical $SEY_{max} \leq 1.9$. Therefore, and according to results in Fig. 5, the ratio of $\lambda_w/\lambda_c \approx 2$. Given the ratio of κ_c/κ_w, the measured tune shift (the order of 10^{-3}) does not show a clear evidence about the presence of the electron cloud in the cold regions. However, the slight assymetry between the vertical and horizontal tunes is a sign of a non-uniform electron density in the beam pipe, and it points towards the presence of an electron density in the arcs. Multipolar magnetic fields present in the arcs create non-uniform electron distribution in the transverse plane, e.g. the "two stripes" measured in presence of dipole fields [7]. This case is still under study. A better estimation of the electron cloud density in the warm part can be done using the data in the electron detectors placed from the warm regions (see Fig. 5, left). The detection of a pressure rise in some cold sections [1] confirms this result.

SUMMARY AND OUTLOOK

The stronger pressure rises detected in the IR regions are consistent with the electron cloud created by the uneven bunch spacings produced by the passage of two beams in the same chamber. The transition and rebucketing pressure rises at STAR are consistent with coming in and out of an electron cloud region in the bunch intensity and bunch length space (N, σ_z). However, how the transition from electron cloud "off" to "on" occurs is still under studies [5], especially for the first order phase transition found in PHOBOS. First results estimating the electron cloud in the cold regions (arcs) using tune shift measurements along the bunch train are introduced, showing that electron cloud can be present in magnetic field regions for due to the observed assymetry in the horizontal vs vertical planes. Results using $CSEC$ show lower electron densities are expected in the regions where the beam pipe radius is smaller. Nevertheless, the introduction of magnetic fields can change this situation and is currently being studied.

ACKNOWLEDGEMENTS

The authors would like to thank K. Harkay (ANL), M. Furman (LBNL), G. Arduini and D. Schulte (CERN), and R. Tomás, J. Gullotta (BNL) for their helpful tips.

REFERENCES

[1] W. Fischer et al. Vacuum pressure rise with intense ion beams in RHIC. Proceedings of ECLOUD'04, Napa, 2004.

[2] U. Iriso et al. BNL C-AD/AP/127 (2003).

[3] S.Y. Zhang et al. PAC'03 proceedings.

[4] G. Rumolo and W. Fischer. BNL C-A/AP/146 (2004).

[5] U. Iriso and S. Peggs. BNL C-AD/AP/147 (2004).

[6] W. Fischer, M. Blaskiewicz, et al. PRST-AB 5, 124401 (2002).

[7] F. Zimmermann, et al. WEPLT044, in these Proceedings.